

ELECTROMAGNETIC FIELDS

PACS numbers: 42.25.Fx; 42.30.Wb; 42.79.Jq
DOI: 10.1070/QE2012v042n01ABEH014769

Localised plasmons on the aperture of a channel in a metal layer

T.I. Kuznetsova, N.A. Raspopov

Abstract. **Optical fields are studied in a planar channel inside a metal layer taking into account a complex dielectric function of the metal. An influence of an exit aperture on the incident field propagating along the channel is considered; a mathematical approach is developed for analysing the effect. Attention is paid to the fact that the incident field should not be assumed *a priori* known if the wave transformation at the exit is neglected. For a chosen dimension of the channel and parameters of a metal, the coefficients for the lowest mode transformation into higher modes are found. The spatial field structure at the exit aperture and on the exit surface of a metal is studied. Existence of domains possessing an anomalously high intensity is revealed.**

Keywords: *nanoscale slit in a metal, planar waveguide modes, wave reflection on an aperture, surface plasmon, singularities of a spatial field structure.*

1. Introduction

Properties of surface plasmons have been widely discussed for last decades. A classical theoretical description of surface plasmons [1] deals with an infinite plane metal–dielectric interface and infinitely wide electromagnetic waves. As opposed to the classical scheme, in real conditions there always exists an initial light beam originated from an external source. In the cases where a wide (as compared to the radiation wavelength) light beam is used for exciting [2, 3], there is a correspondence between plasmon characteristics of real and idealised schemes.

The situation is quite different if the exciting beam cross section is comparable to the radiation wavelength. In a series of recent investigations, the initiating field was produced by means of a narrow channel in a metal plate. In [4], the cylindrical channel was considered; in [5, 6] the channel was planar. We will not discuss a wide range of works originated from [7], which consider periodical systems of channels or holes in metal films. The ideas initiated by those works influenced numerous studies in nanostructure optics. However, our work is not directly connected with periodical systems, and we will only discuss the cases of single channels.

Characteristics of surface plasmons excited by the fields formed in channels were theoretically discussed in [8, 9, 10]. Attention was paid to certain features of plasmon behaviour under localised excitation; in particular, the character of plasmon attenuation was investigated at large distances from the excitation point [9]. It is substantial that in most of the works it is assumed that employment of the Green tensor (Green function) guarantees obtaining a rigorous solution. However, the Green function employed in those works does not match field boundary conditions on the walls. Thus, the solution is *a fortiori* approximate and completeness of the physical picture resulting from the solution is not obvious.

Here we will pay attention to specific features of eigenwaves for the channel and consider transformation of the eigenwaves as they exit from the channel to a free space. We will not consider transformation of the initial field on an input plane. We assume that a single wave with a lowest attenuation survives in the channel, which corresponds to the case where the metal plate thickness is not too small. The wave at the exit plane transforms into various reflected waves that are channel eigenwaves.

Note that formation of the exciting light beam and origin of surface waves on the output plane are closely interrelated and should be considered jointly. Such approach provides obtaining a detailed picture of the exit field both far from the excitation localisation region and at short distances from the channel, including the output hole itself.

2. Eigenwaves for a channel in the medium possessing dielectric characteristics of a real metal

Characteristics of eigenwaves in a plane uniform layer are calculated by well-known methods. In particular, such methods employed for calculating optical fields in planar waveguides are presented in monograph [11]. Below we will briefly discuss a method in the form convenient for further employment. Consider a uniform layer (air for simplicity) inside a metal. The layer thickness is $2a$. We assume the dielectric function ε of the metal constant with a negative real part and positive imaginary part. We will consider TM-modes only. In this case, there are three field components, namely, $\tilde{H}_y$, $\tilde{E}_x$, $\tilde{E}_z$. The components $\tilde{E}_x$ and $\tilde{E}_z$ can be expressed in terms of the component $\tilde{H}_y$ as follows

T.I. Kuznetsova, N.A. Raspopov P.N. Lebedev Physics Institute, Russian Academy of Sciences, Leninsky prosp. 53, 119991 Moscow, Russia; e-mail: tkuzn@sci.lebedev.ru, rna@sci.lebedev.ru

Received 14 November 2011
Kvantovaya Elektronika **42** (1) 87–94 (2012)
Translated by N.A. Raspopov

$$\tilde{E}_x = \frac{-\mathrm{i}}{\omega/c}\frac{\partial}{\partial z}\tilde{H}_y\begin{bmatrix}1, & |x|\leqslant a\\ 1/\varepsilon, & |x|>a\end{bmatrix}, \quad (1)$$

$$\tilde{E}_z = \frac{-\mathrm{i}}{\omega/c}\frac{\partial}{\partial x}\tilde{H}_y\begin{bmatrix}1, & |x|\leqslant a\\ 1/\varepsilon, & |x|>a\end{bmatrix}. \quad (2)$$

The time dependence is assumed harmonic with the light field frequency ω, c is the speed of light, and the coordinate axes are shown in Fig. 1. We will only consider even modes and take the expression for the magnetic field in the form

$$\tilde{H}_y = \mathrm{const}\exp(-\mathrm{i}\omega t + \mathrm{i}kz) \times\begin{bmatrix}\cos(qx), & |x|\leqslant a\\ \cos(qa)\exp[-p(|x|-a)], & |x|>a\end{bmatrix}. \quad (3)$$

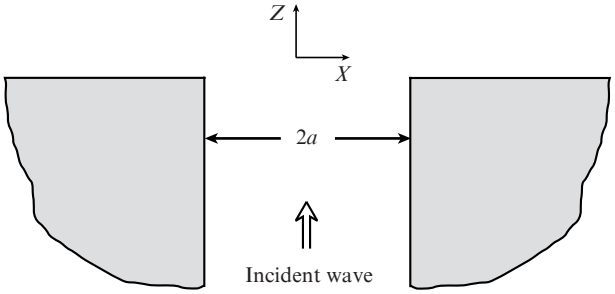

Figure 1. Scheme of a channel in a bulk metal used for calculating fields.

Here the wave vectors and frequency are related by the obvious relationship

$$q^2 + k^2 = \frac{\omega^2}{c^2}, \quad -p^2 + k^2 = \varepsilon\frac{\omega^2}{c^2}. \quad (4)$$

The magnetic permeability is taken equal to unity for the whole system; therefore, the magnetic field component is continuous on all interface surfaces. The continuity of the field $\tilde{H}$ at the channel boundaries is guaranteed by above given expression (3). The dependence of the magnetic field on the coordinate x (3) may be expressed in terms of the function φ determined as follows

$$\varphi(x) = \begin{bmatrix}\cos(qx), & |x|\leqslant a\\ \cos(qa)\exp[-p(|x|-a)], & |x|>a\end{bmatrix}. \quad (5)$$

We may also introduce the function ψ for the component $\tilde{E}_x$

$$\psi(x) = \begin{bmatrix}\cos(qx), & |x|\leqslant a\\ \frac{1}{\varepsilon}\cos(qa)\exp[-p(|x|-a)], & |x|>a\end{bmatrix}. \quad (6)$$

These notations result in the following expressions for the field components

$$\tilde{H}_y = \mathrm{const}\varphi(x)\exp(-\mathrm{i}\omega t + \mathrm{i}kz), \quad (7)$$

$$\tilde{E}_x = \mathrm{const}\frac{ck}{\omega}\psi(x)\exp(-\mathrm{i}\omega t + \mathrm{i}kz), \quad (8)$$

$$\tilde{E}_z = \mathrm{const}\frac{\mathrm{i}c}{\omega}\frac{\partial}{\partial x}\psi(x)\exp(-\mathrm{i}\omega t + \mathrm{i}kz). \quad (9)$$

The choice of the functions φ and ψ provides that (1) holds and guarantees continuity of the magnetic field and the normal component of electric induction at the channel boundary. Expression (9) should provide continuity of the component $\tilde{E}_z$ at the channel–metal interface, which imposes a constraint on the value of the transversal component of the wave vector q, namely, the value of q should satisfy the equation

$$\varepsilon q\sin(qx)|_{x=a} = p\cos(qa)\exp[-p(|x|-a)]|_{x=a}. \quad (10)$$

By combining (10) and (4), we obtain the equation for finding the parameters q and p. In what follows, we will consider the dimensionless parameters

$$Q = qa,\ P = pa,\ W = (\omega/c)a,\ K = ka = \sqrt{W^2 - Q^2}. \quad (11)$$

In these notations we find from (10) and (4)

$$\varepsilon Q\tan Q = P, \quad (12)$$

$$P^2 = (1-\varepsilon)W^2 - Q^2 \quad (13)$$

or, combining (12) and (13) we finally obtain

$$\varepsilon Q\tan Q = \sqrt{(1-\varepsilon)W^2 - Q^2}. \quad (14)$$

By solving (14), we obtain the values of the dimensionless wave vector in the channel and the exponential power (6) in a metal (Q and P). This calculation scheme coincides with the traditional scheme known from literature. Differences are connected with the dielectric characteristics of the medium that will be employed in solving (14) and with the fact that we will consider not only real but also complex wave vectors. Recall that in the case of an ideal metal ($|\varepsilon|\to\infty$), the eigenvalues for the wave vectors are real equidistant numbers $Q_n = n\pi$, $n = 0, 1, 2, \ldots$. In the case of a real negative dielectric function, only several first eigenvalues are real numbers and the rest are complex values. If we pass to a dissipative metal ($\mathrm{Re}(\varepsilon) < 0$, $\mathrm{Im}(\varepsilon) > 0$) then all eigenvalues become complex. In this case, if Q is an eigensolution, then $-Q$ is eigensolution as well. If the imaginary part of the dielectric function equals zero, then for every solution Q' there exist, in addition to the solution $-Q'$, solutions $\pm(Q')^*$.

However, if the imaginary part of the dielectric function ε is distinct from zero, then the complex conjugated values will no longer be solutions. Here, we consider the solutions with a positive real part of Q as main solutions. In the case of a real dielectric function ε, for the main solution we take the solution with $\mathrm{Re}(Q)\mathrm{Im}(Q) < 0$. In this case, the wave damps with a distance from the channel axis [the inequality $\mathrm{Re}(P)\mathrm{Im}(P) > 0$) holds]. In addition, in this case the waves propagating along the channel damp in the propagation direction [$\mathrm{Re}(K)\mathrm{Im}(K) > 0$].

In the case of a complex dielectric function, the situation is more complicated. The waves corresponding to eigenvalues

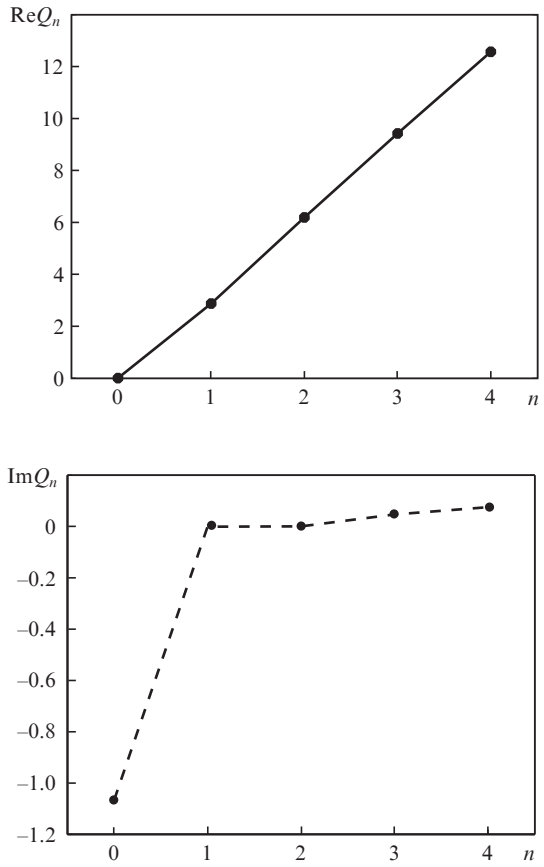

Figure 2. First five roots of Eqn (14) for the case $\varepsilon = -10 + 0.1\mathrm{i}$.

with large numbers (in our example with $n > 2$) increase in the direction of the wave vector. The intensity of the light flux calculated in the channel increases in the direction of the energy flux along the channel axes. For example, first five eigenvalues are presented in Fig. 2 for the case of the complex dielectric function $\varepsilon = -10.0 + 0.1\mathrm{i}$. In what follows, only such 'inconvenient' waves will be considered.

There is a remark concerning properties of solutions in the case of a complex dielectric function. One may show that Eqn (14) has an infinite number of solutions. Indeed, consider a case of large values of Q. Let

$$|Q^2| \gg |(1-\varepsilon)W^2|. \tag{15}$$

If (15) holds, then (14) reduces to the following:

$$\varepsilon Q \tan(Q) = -\mathrm{i}Q. \tag{16}$$

This entails

$$\frac{\exp(\mathrm{i}Q) - \exp(-\mathrm{i}Q)}{\exp(\mathrm{i}Q) + \exp(-\mathrm{i}Q)} = \frac{1}{\varepsilon} \tag{17}$$

and we may find the explicit solution

$$Q = n\pi + b, \quad b = \frac{\mathrm{i}}{2}\ln\frac{1-\varepsilon}{-1-\varepsilon}. \tag{18}$$

In the case of $\varepsilon = -10.0 + 0.1\mathrm{i}$ (see Fig.2), we obtain from (18) $Q_n = n\pi - 0.001010 + 0.100325\mathrm{i}$. Note that the asymptotic is only valid at sufficiently large numbers ($n \approx 40$). The number n in (18) can be infinitely increased: $n = n_{\min} + 1, n_{\min} + 2, n_{\min} + 3, \ldots$ We only have to take large numbers ($n > n_{\min} = 40$) in order to satisfy condition (15), which was used in reducing Eqn (14) to the form (16). Hence, we obtain an infinite set of values Q_n that are solutions to the initial equation (14). Each root Q_n corresponds to the wavenumber P_n in a metal determined by formula (13) and to the value K_n determined by formulae (4) and (11). Also, to each root Q_n we will put in correspondence the function φ of type (5) responsible for the magnetic field and the function ψ of type (6) referring to the field component E_x. Earlier, by using formulae (11) we passed to dimensionless wavenumbers. It will be also convenient to introduce the dimensionless coordinates

$$X = x/a, \quad Z = z/a. \tag{19}$$

In these coordinates the functions φ and ψ take the form

$$\varphi_n(X) = \begin{bmatrix} \cos(Q_n X), & |X| \leqslant 1 \\ \cos(Q_n)\exp[-P_n(|X|-1)], & |X| < 1 \end{bmatrix}, \tag{20}$$

$$\psi_n(X) = \begin{bmatrix} \cos(Q_n X) & |X| \leqslant 1 \\ \dfrac{1}{\varepsilon}\cos(Q_n)\exp[-P_n(|X|-1)], & |X| > 1 \end{bmatrix}. \tag{21}$$

Consideration of waves for an infinite planar waveguide is only an auxiliary task. Our aim is to study a semi-infinite planar waveguide having an interface with free space.

3. Waveguide field transformation at an exit from a planar waveguide to free space

Let us consider transformation of the wave propagating along the channel as it reflects from a metal–free space interface. In describing such transformation, we should satisfy boundary conditions for the field in the plane $Z = 0$ (see Fig. 1). For this, we need to include into the consideration all waves that may propagate across the infinite waveguide. We may present a total field in the channel as a linear combination of various eigenwaves. For shortness, we drop the time factor $\exp(-\mathrm{i}\omega t)$ and transfer to the new notations for the field components H_y, E_x, E_z related with the previous components $\tilde{H}_y, \tilde{E}_x, \tilde{E}_z$ by the relationships

$$\tilde{H}_y = H_y \exp(-\mathrm{i}\omega t),$$

$$\tilde{E}_x = E_x \exp(-\mathrm{i}\omega t), \tag{22}$$

$$\tilde{E}_z = E_z \exp(-\mathrm{i}\omega t).$$

We may write the field component H_y in the form

$$H_y(X,Z) = \sum_{n=0}^{\infty}[\delta_{n0}\alpha_{\mathrm{inc}}\exp(\mathrm{i}K_n Z) + \alpha_n \exp(-\mathrm{i}\eta_n K_n Z)]\varphi_n(X), \quad Z < 0. \tag{23}$$

Here $K_n = \sqrt{W^2 - Q_n^2}$; δ_{n0} is the Kronecker symbol. This means that a wave with the structure of the zero mode and

with the amplitude α_{inc} passes to the system from negative values of z. Amplitudes of all other waves are unknown and should be found. The sign of the product $\text{Re}(Q)\text{Im}(Q)$ determines the factor η_n. We assume

$$\eta_n = 1, \quad \text{Re}(Q_n)\text{Im}(Q_n) < 0, \qquad \eta_n = -1, \quad \text{Re}(Q_n)\text{Im}(Q_n) > 0. \tag{24}$$

The choice of the sign is related to the fact that for the reflected waves we take the waves that damp with a distance from the metal–free space interface. In Section 1, we have mentioned that only for a few first modes the wave propagation direction along the channel axis coincides with the direction of the wave amplitude damping. Condition (24) means that among reflected waves we prefer the direction of damping rather than the direction of the wave front motion. This preference determines the appearance of the reflected waves that we have chosen in writing (23). The expressions for the field components E_x and E_z are as follows

$$E_x(X,Z) = \sum_{n=0}^{\infty} \frac{K_n}{W}[\delta_{n0}\alpha_{\text{inc}}\exp(\text{i}K_nZ) - \eta_n\alpha_n\exp(-\text{i}\eta_nK_nZ)]\psi_n(X), \qquad Z \leqslant 0, \tag{25}$$

$$E_z(X,Z) = \sum_{n=0}^{\infty} \frac{1}{\text{i}W}[\delta_{n0}\alpha_{\text{inc}}\exp(\text{i}K_nZ) + \alpha_n\exp(-\text{i}\eta_nK_nZ)]\Big[-\frac{\partial}{\partial X}\psi_n(X)\Big], \qquad Z \leqslant 0. \tag{26}$$

Now we may write expressions for the field components in a free space outside a metal $Z > 0$. The fields $E_x^{\text{out}}, H_y^{\text{out}}$ should be continuations of the fields E_x and H_y determined by (25) and (26).

We may introduce the Fourier transforms of functions φ_n and ψ_n:

$$\varphi_n(X) = \int_0^{\infty} \Phi_n(\varkappa)\cos(\varkappa X)\text{d}\varkappa, \qquad \Phi_n(\varkappa) = \frac{2}{\pi}\int_0^{\infty} \varphi_n(X)\cos(\varkappa X)\text{d}X, \tag{27}$$

$$\psi_n(X) = \int_0^{\infty} \Psi_n(\varkappa)\cos(\varkappa X)\text{d}\varkappa, \qquad \Psi_n(\varkappa) = \frac{2}{\pi}\int_0^{\infty} \psi_n(X)\cos(\varkappa X)\text{d}X; \tag{28}$$

note that $\varphi(X)$ and $\psi(X)$ are even functions. The component E_x^{out} in a free space is written in the form:

$$E_x^{\text{out}}(X,Z) = \int_0^{\infty}\sum_{n=0}^{\infty} \frac{K_n}{W}(\delta_{n0}\alpha_{\text{inc}} - \eta_n\alpha_n)\times \Psi_n(\varkappa)[\exp(\text{i}\sqrt{W^2-\varkappa^2}\,Z)]\cos(\varkappa X)\text{d}\varkappa, \quad Z > 0. \tag{29}$$

At the boundary $Z = 0$ the fields $E_x(X)$ and $E_x^{\text{out}}(X)$ coincide; the field E_x^{out} comprises only outgoing or damping waves as $Z \to \infty$. Using the expression for $E_x^{\text{out}}(X, Z)$, in accordance with the Maxwell equations, we may derive the expression for the field $H_y^{\text{out}}(X, Z)$:

$$H_y^{\text{out}}(X,Z) = \int_0^{\infty}\sum_{n=0}^{\infty} \frac{K_n}{W}(\delta_{n0}\alpha_{\text{inc}} - \eta_n\alpha_n)\,\Psi_n(\varkappa) \times\frac{W}{\sqrt{W^2-\varkappa^2}}[\exp(\text{i}\sqrt{W^2-\varkappa^2}\,Z)]\cos(\varkappa X)\text{d}\varkappa, \quad Z > 0. \tag{30}$$

Now we may write the equality condition for the fields H_y^{out} and H_y at $Z = 0$:

$$H_y^{\text{inner}}(X,0) = H_y^{\text{out}}(X,0). \tag{31}$$

Here, the superscript 'inner' refers to a field in the channel. Taking into account (23) and (30) we may rewrite (31) in the form

$$\sum_{n=0}^{\infty}(\delta_{n0}\alpha_{\text{inc}} + \alpha_n)\varphi_n(X) = \int_0^{\infty}\sum_{n=0}^{\infty} \frac{K_n}{W}(\delta_{n0}\alpha_{\text{inc}} - \eta_n\alpha_n) \times \Psi_n(\varkappa)\frac{W}{\sqrt{W^2-\varkappa^2}}\cos(\varkappa X)\text{d}\varkappa. \tag{32}$$

Since equality (32) holds for all X we may multiply its both sides by an arbitrary function of X and the equality would remain valid. Then we may integrate the result over X, the equality still remaining valid. We will perform these procedures using the functions ψ_m^*. Reasonability of such approach was established in our previous works in similar subject [12, 13], in which, however, we considered different geometry and material constants. After performing the above procedures we obtain

$$\sum_{n=0}^{\infty}(\delta_{n0}\alpha_{\text{inc}} + \alpha_n)\langle\varphi_n\psi_m^*\rangle = \int_0^{\infty}\sum_{n=0}^{\infty} \frac{K_n}{W}(\delta_{n0}\alpha_{\text{inc}} - \eta_n\alpha_n) \times \Psi_n(\varkappa)\langle\cos(\varkappa X)\psi_m^*\rangle\frac{W}{\sqrt{W^2-\varkappa^2}}\text{d}\varkappa. \tag{33}$$

Here

$$\langle\varphi_n\psi_m^*\rangle = \int_0^{\infty}\varphi_n(X)\,\psi_m^*(X)\text{d}X; \tag{34}$$

$$\langle\cos(\varkappa X)\psi_m^*\rangle = \int_0^{\infty}\cos(\varkappa X)\,\psi_m^*(X)\text{d}X. \tag{35}$$

In view of (28) for the Fourier transforms we may write

$$\langle\cos(\varkappa X)\psi_m^*\rangle = \frac{\pi}{2}\,\Psi_m^*(\varkappa). \tag{36}$$

By using (36) we may write (33) in the form

$$\sum_{n=0}^{\infty}(\delta_{n0}\alpha_{\text{inc}} + \alpha_n)\langle\varphi_n\psi_m^*\rangle = \frac{\pi}{2}\int_0^{\infty}\sum_{n=0}^{\infty} \frac{K_n}{W}(\delta_{n0}\alpha_{\text{inc}} - \eta_n\alpha_n)\times$$

$$\times \Psi_n(\varkappa)\,\Psi_m^*(\varkappa)\frac{W}{\sqrt{W^2-\varkappa^2}}\,\mathrm{d}\varkappa. \tag{37}$$

The values of $\langle\varphi\psi^*\rangle$ and functions Ψ included in (33) can be directly calculated; the calculations give

$$\langle\varphi_n\psi_m^*\rangle = \frac{1}{2}\frac{\sin(Q_n-Q_m^*)}{Q_n-Q_m^*}+\frac{1}{2}\frac{\sin(Q_n+Q_m^*)}{Q_n+Q_m^*}$$
$$+\frac{\cos(Q_n)\cos(Q_m^*)}{\varepsilon^*}\frac{1}{P_n+P_m^*}, \tag{38}$$

$$\Psi_n(\varkappa) = \frac{1}{\pi}\Big[\frac{1}{2}\frac{\sin(Q_n-\varkappa)}{Q_n-\varkappa}+\frac{1}{2}\frac{\sin(Q_n+\varkappa)}{Q_n+\varkappa}$$
$$+\frac{1}{\varepsilon}\cos(Q_n)\frac{P_n\cos\varkappa-\varkappa\sin\varkappa}{P_n^2+\varkappa^2}\Big]. \tag{39}$$

For shortness, we may introduce the following notations:

$$C(n,m) = \langle\varphi_n\psi_m^*\rangle, \tag{40}$$

$$B(n,m) = \frac{\sqrt{W^2-Q_n^2}}{W}\frac{\pi}{2}\int_0^\infty \Psi_n(\varkappa)\,\Psi_m^*(\varkappa)\frac{W}{\sqrt{W^2-\varkappa^2}}\mathrm{d}\varkappa. \tag{41}$$

In these notations, formula (37) takes the form

$$\sum_{n=0}^{\infty}\alpha_n[C(n,m)+\eta_n B(n,m)] = \alpha_{\mathrm{inc}}[B(0,m)-C(0,m)]. \tag{42}$$

The equality obtained (42) is an infinite set of equations (m = 0,1,2,…) for an infinite number of variables (α_0, α_1, α_2,…). After the values (α_0, α_1, α_2,…) are found, one may construct the distribution of fields in the channel, free space, and, surely, on the metal–free space interface.

4. Calculation results: filed features at the exit from the channel to a free space

The system of equations (42) was solved numerically. The dielectric function was chosen with a large negative real part and a small dissipation (ε = –10.0 + 0.1i); the channel width was taken so that $2a = 0.8\lambda$, i.e., $W = 0.8\pi$ (λ is the radiation wavelength). In the calculations, we assumed $\alpha_{\mathrm{inc}} = 1$. A truncated system of equations was solved. Variants with various numbers of unknowns α_n (and the corresponding numbers of equations) were tested, the maximal value was $n = 96$. A relative difference for α_n calculated by solving the sets of 48 and of 96 equations did not exceed 0.01. Absolute values and real and imaginary parts of the coefficients α_n are shown in Fig. 3 versus number n. One can see that the absolute values of the coefficients α_n decrease with the number n as $1/n$. In the strict sense, the accuracy of this dependence requires additional study. It is possible that at higher precision of solving the system of equations (42) this dependence may change; we admit that an asymptotic law of the type $\alpha_n \propto n^{-(1+\mu)}$, may be obtained, where $1 \gg \mu > 0$. Here, we will take $\mu = 0$. One should note phase jumps are obtained in the coefficients α_n for neighbouring numbers.

The obtained coefficients α_n give complete information about the field structure in space [formulae (23), (25), (26)]. The far-field zone picture is determined by the Fourier transform of a field, which for every particular mode is given by formula (39). With the parameters chosen in our case, there exists a single maximum in the far-field zone, which corresponds to the zero angle. Its half-height half-width found from numerical estimates is ~30°. At the channel width greater than 0.8λ, we obtained additional side maxima around the central peak.

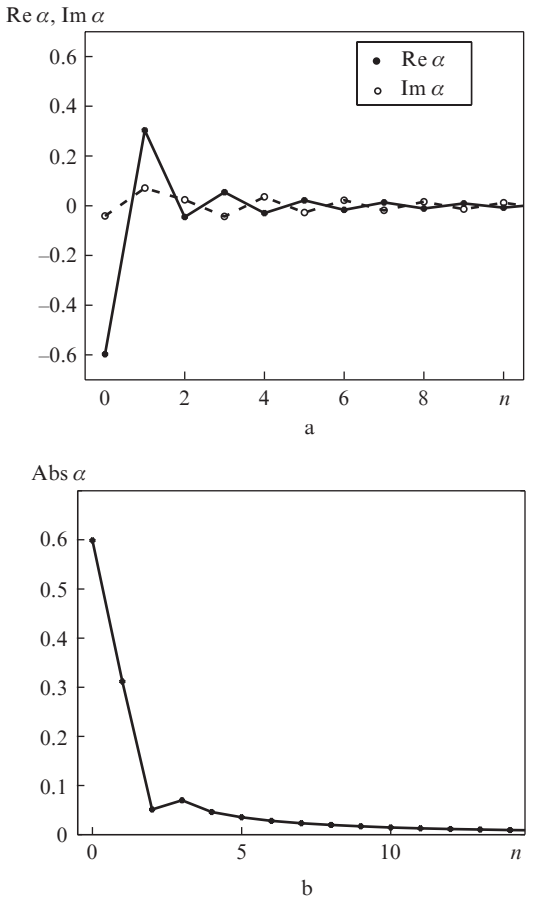

Figure 3. Real and imaginary parts (a) and absolute value (b) of the coefficients $\alpha(n)$.

The structure of the near-field picture is more complicated. Consider fields in the plane $Z = 0$. The absolute value of the component E_x versus coordinate X is shown in Fig. 4. In plotting the curves we assume the amplitude of the incident wave field component E_x unity, hence α_{inc} obeys the condition

$$\alpha_{\mathrm{inc}}\frac{K_0}{W} = 1. \tag{43}$$

A sharp amplitude spike is seen in Fig. 4 at $X = \pm 1$, i.e., at the channel exit edge. For example, at $X = 1$, $Z = 0$, the calculated absolute value of E_x is 12 times greater than that of the field passing from infinity along the channel. Recall that the field amplitude is discontinuous at the point $X = 1$. Approaching this point from the right gives the field amplitude less than the mentioned value by a factor of $|\varepsilon|$. Due to such behaviour of the field amplitudes, we may speak of localised plasmons arising in the system under consideration. If we turn to the range $X > 1$, we can see a series of noticeable peaks at points $X = \pm 3, \pm 5, \pm 7, \ldots$ Intensity of the peaks falls

with a distance from the channel. Such a series of peaks corresponds to wave reflection from the channel walls. Consider the behaviour of fields near the mentioned specific points in more detail. A thorough investigation requires taking into account a contribution from modes with higher numbers ($n \geqslant 96$). However, we may draw some conclusions without performing additional calculations by using the asymptotic behaviour found for the coefficients.

5. Singular points in the spatial structure of a field

In plotting the curves in Fig. 4, we have made allowance for a contribution of waves with numbers $n < 96$. As was mentioned above, at high mode numbers the coefficients of magnetic field expansion obey the dependence $\alpha_n \sim n^{-1}$. Hence, the expansion coefficients for the x-component of electric field (E_x) have an asymptotically constant absolute value [see (11) and (18) for the wave vectors and (25) for the field]. It is clear that nondecreasing coefficients in the field expansion would result in unlimited amplitudes of the field at some points of space. In further analysis of specific features of field structures, it will be convenient to use expansion coefficients for the field component E_x. For this purpose, we introduce new coefficients β_n instead of α_n

$$\beta_n = -\eta_n \frac{K_n}{W}\alpha_n. \tag{44}$$

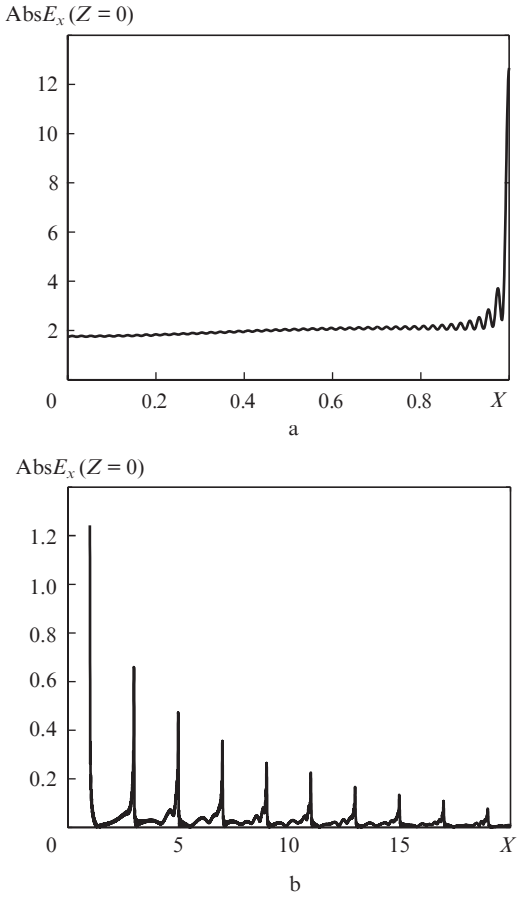

Figure 4. The field component E_x in the plane $Z = 0$ over segment $0 \leqslant X \leqslant 1$ (at the exit aperture) (a) and at $1 \leqslant X$ (b).

The dependence of $|\alpha_n|$ on n mentioned above and the phase characteristics for these coefficients obtained make it possible to present β_n at $n \gg 1$ in the form

$$\beta_n = -\beta_\infty(-1)^n. \tag{45}$$

As for the initial parameter β_{inc}, we will, in a similar manner [see (43)], assume that the incident wave passing along the channel from negative Z values has the component E_x of unity amplitude, that is,

$$\beta_{\text{inc}} \equiv \frac{K_0}{W}\alpha_{\text{inc}} = 1. \tag{46}$$

For this value of β_{inc} the calculations give $\beta_\infty \approx 0.05 + 0.05\text{i}$.

Now we may estimate the field basing on an infinite set of coefficients β_n. For shortness, we will only consider the range $|X| \leqslant 1$, $Z < 0$. We may transfer formula (25) by replacing the coefficients α_n with β_n according to (44) and using expressions of type (21) for the spatial dependence of functions ψ_n at $|X| \leqslant 1$ and dividing the infinite sum into two sums. Then we obtain

$$E_x(X,Z) = \sum_{n=0}^{N}[\delta_{n0}\exp(\text{i}K_nZ) + \beta_n\exp(-\text{i}\eta_nK_nZ)]\cos(Q_nX) + \sum_{n=N+1}^{\infty}\beta_n\exp(-\text{i}\eta_nK_nZ)\cos(Q_nX). \tag{47}$$

Now we pass to approximate calculations: in the second sum in (47), we may replace the parameters β_n, Q_n and $K_n = \text{i}\sqrt{Q_n^2 - W^2}$ with their asymptotic values. In this case, the exact equality (47) transfers to the following approximate expression

$$E_x(X,Z) = \Sigma_N^{(E_x)} + (\sigma_\infty^{(E_x)} - \sigma_N^{(E_x)}). \tag{48}$$

Here the finite sum from (47) is denoted by $\Sigma_N^{(E_x)}$ (no approximations are made):

$$\sigma_\infty^{(E_x)} = \beta_\infty\sum_{n=0}^{\infty}(-1)^n\cos[(\pi n + b)X]\exp[(\pi n + b)Z]; \tag{49}$$

$$\sigma_N^{(E_x)} = \beta_\infty\sum_{n=0}^{N}(-1)^n\cos[(\pi n + b)X]\exp[(\pi n + b)Z]. \tag{50}$$

By summing the series included in (49), we obtain [14]

$$\sigma_\infty^{(E_x)} = \beta_\infty\cos(bX)\text{e}^{bZ}\frac{\text{e}^{\pi Z}\cos(\pi X) + 1}{1 + 2\text{e}^{\pi Z}\cos(\pi X) + \text{e}^{2\pi Z}} + \beta_\infty\sin(bX)\text{e}^{bZ}\frac{\text{e}^{\pi Z}\sin(\pi X)}{1 + 2\text{e}^{\pi Z}\cos(\pi X) + \text{e}^{2\pi Z}}. \tag{51}$$

Note that we operate with $Z < 0$, and convergence of the series in (49) is guaranteed.

Consider a vicinity of point $Z = 0$, $X = 1$. Let $X = 1 - \xi$, $Z = -\zeta$, where ξ, ζ are positive and $\xi, \zeta \ll 1$. Then we have

$$\lim_{\xi \to 0, \zeta \ll \xi} \sigma_{\infty}^{(E_x)} = \beta_{\infty} e^{bZ}$$

$$\times \frac{1}{\pi}\left[\cos(bX)\frac{\zeta}{\xi^2 + \zeta^2} - \sin(bX)\frac{\xi}{\xi^2 + \zeta^2}\right]. \quad (52)$$

By presenting the delta-function as the limit of continuous functions (see [15]) and taking into account that expansion (49) is only valid at $|X| \leqslant 1$ whereas at other values of X the field is given by another expression, we obtain the following result. Under the condition $\zeta \ll \xi$, $\xi \to 0$ formula (52) takes the form

$$\lim_{\xi \to 0, \zeta \ll \xi} \sigma_{\infty}^{(Ex)} = \beta_{\infty} e^{bZ}$$

$$\times \left[\frac{1}{2}\cos(bX)\delta(1 - X) - \sin(bX)\frac{1}{\pi}\frac{1}{1 - X}\right]. \quad (53)$$

Expression (53) presents the component E_x near the singular point in the form that will be observed while approaching the point along the line $Z = 0$.

Similar transformations may be performed for the case $\xi \ll \zeta$, $\zeta \to 0$, which would give the field while approaching the edge along a channel wall. Thus, this is one more evidence that the component E_x has a singularity at the point $X = 1$, $Z = 0$.

Similar transformations allow one to separate singular summands in the expressions for the field components #Hy and E_z. The forms of these summands show that the component E_z has singularities of the same type as E_x, and the magnetic field increases in a vicinity of the point $X = 1$ slower than the electric field. Only a vector potential will have no singularities.

The result presented should be compared to known solutions of electrostatic problems [16, 17]. In [16], a field near an edge of a perfect conductor is considered, and in [17], a field is studied in the case of two edges, i.e, actually at an exit from a channel in a perfect conductor. It is shown [16, 17] that in the case of normal angles between metal surfaces the electric field increases near the edge as $(\xi^2 + \zeta^2)^{-1/6}$, whereas the potential is described by $(\xi^2 + \zeta^2)^{1/3}$, where $(\xi^2 + \zeta^2)^{1/2}$ is the distance from an observation point to the edge. The distinction is related to the fact that in the mentioned monographs the fields were forced to vanish at infinity, whereas we do not impose such a constraint. Conversely, our scheme includes a wave passing along the channel from negative values of z.

We have considered singular points in the field structure in the range $|X| \leqslant 1$. Analysis of the range $|X| > 1$ reveals a series of infinitely intensive peaks at the metal–free space interface at the points $X = \pm 3, \pm 5, \pm 7, \ldots$ In real conditions, this effect is partially suppressed due to smooth edges and surface roughness. If the surface is not perfect, the phase relationships between spatial harmonics break, which results in a spread of maxima. One may take that at the dimension of nonuniformities of the order of λ/m, only the waves with the wavenumbers less than m/λ (that is, with the numbers $n < ma/\lambda$) would constructively interfere. In this case, in estimating the field value one should take into account a contribution of a finite number of harmonics with the numbers less than ma/λ. Our estimation in Section 4 based on the calculation of a finite sum corresponds to the irregularity scale of the order of $\sim\lambda/100$.

6. Conclusions

Wavenumbers are obtained for fields in a planar channel inside a real metal. For low-number modes ($n < 96$) the wavenumbers are found from numerical calculations, and for higher-order modes the asymptotic formulae are obtained.

The theoretical description is given for the light field transformation at the exit from the channel to a free space. The transformation includes possible mode reflection or transformation into modes with distinct numbers.

The numerical values of the coefficients are obtained for transformation of the incident lower mode into modes of higher numbers for a chosen channel width, wavelength, and dielectric function.

The calculations relevant to the field transformation on the exit aperture are based on the developed mathematical approach; it is essential that method applicability does not require orthogonality of channel eigenmodes (note that there is no orthogonality if medium is absorbing).

Singular points are found in the spatial structure of field in the exit plane. The field amplitude exhibits abrupt peaks at these points. The most noticeable amplitude discontinuity occurs at the exit aperture edge, which corresponds to the points ±1 in our notations. Such singular points have an analogue in the electrostatic of ideal conductors. It is important that making allowance for real dielectric characteristics of a metal does not abandon this effect. In the case of imperfect shapes of metal surfaces, the effect weakens and maxima spread, however, do not vanish. The field on the exit metal plane has a series of equidistant bright points in which the field intensity falls with a distance from the output aperture. Thus, one may speak about localised plasmons arising on the surface.

Acknowledgements. The work was supported by the Russian Foundation for Basic Researches (Grant No. 10-02-00795-a). The authors are grateful to V.S. Lebedev, A.V. Masalov, and A.G. Vitukhnovsky for useful discussions.

References

1. Raether H. *Surface Plasmons on Smooth and Rough Surfaces and on Gratings* (Berlin: Springer-Verlag, 1988).
2. Otto A. *Z. Phys*., **216**, 398 (1968).
3. Kretschmann E. *Z. Phys.,* **241**, 313 (1971).
4. Laluet J.-Y., de Leon-Perez F., Mauboub O., Hohenau A., Ditlbacher H., Garcia-Vidal F.J., Dintinger J., Ebbesen T.W., Martin-Moreno L., Krenn J.R. *Opt. Express,* **16**, 3420 (2008).
5. Baudrion A.-K., Drezet A., Genet C., Ebbesen T.W. *New J. Phys*., **10**, 105014 (2008).
6. Kihm H.W., Lee K.G., Kim D.S., Ahn K.J. *Opt. Commun*., **282**, 2442 (2009).
7. Ebbesen T.W., Lezec H.J., Graemi H.F., Thio T., Wolff P.A. *Nature (Ldn),* **391**, 667 (1998).
8. Dai W., Soukoulis C.M. *Phys. Rev. B*, **80** (15), 155407 (2009).
9. Nikitin A.Yu., Rodrigo S.G., Garcia-Vidal F.J., Martin-Moreno L. *New J. Phys*., **11**, 123020 (2009).
10. Nikitin A.Yu., Garcia-Vidal F.J., Martin-Moreno L. *Phys. Stat. Sol. RRL,* **4** (10), 250 (2010).

11. Adams M.J. *An Introduction to Optical Waveguides* (New York: Wiley 1981; Moscow: Mir 1984).
12. Kuznetsova T.I., Lebedev V.S. *Phys. Rev. B,* **70**, 035107 (2004).
13. Kuznetsova T.I., Lebedev V.S. *Phys. Rev. E*, **78**, 016607 (2008).
14. Prudnikov A.P., Brychkov Yu.A., Marichev O.I. *Integraly i ryady* (Integrals and Series) (Moscow: Nauka 1981) Vol. 1, p. 739.
15. Korn G.A., Korn T.M. *Mathematical Handbook for Scientists and Engineers* (London: McGraw, 1961; Moscow: Nauka 1970).
16. Landau L.D., Lifshitz E.M. *Electrodynamics of Continuous Media* (Oxford: Pergamon Press, 1984; Moscow: Nauka, 1982).
17. Smirnov V.I. *Kurs vysshei matematiki* (A course in Higher Mathematics) (Moscow: Gos. Izd. Tekhniko-Teoreticheskoi Literatury, 1953) Vol. 3, Ch. 2.